

Figure 1. Carboxylation extent dependence of number distribution $f_n(R_h)$ of hydrodynamic radius of CSEBS nanoparticles, where $C = 1.0 \times 10^{-5}$ g/mL.

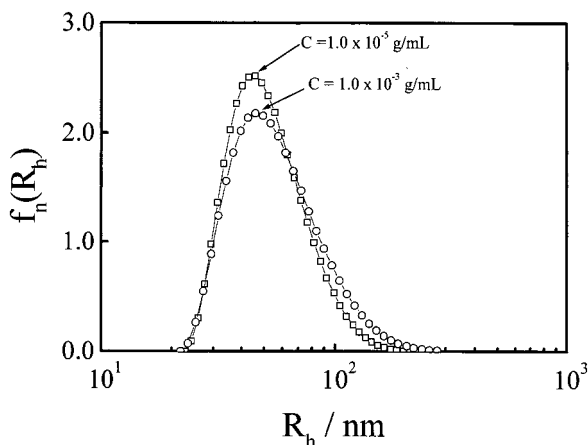


Figure 2. Concentration dependence of number distribution $f_n(R_h)$ of hydrodynamic radius of CSEBS nanoparticles, where $[-\text{COOH}] = 13.3$ mol % and $C = 1.0 \times 10^{-5}$ g/mL.

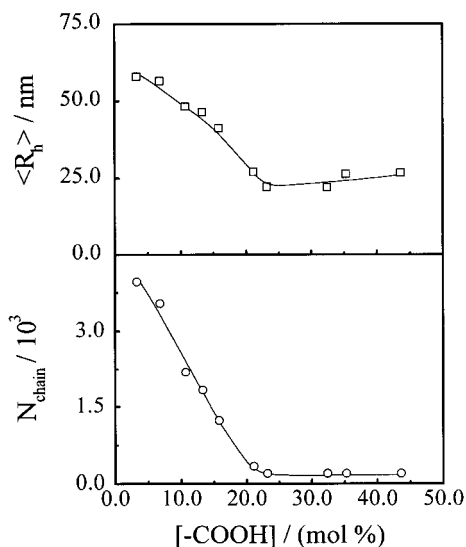


Figure 3. Carboxylation extent dependence of average hydrodynamic radius ($\langle R_h \rangle$) of CSEBS nanoparticles and average number (N_{chain}) of polymer chains inside, where $C = 1.0 \times 10^{-5}$ g/mL and N_{chain} is defined as $M_{w,\text{particle}}/M_{w,\text{chain}}$.

state laser (ADLAS DPY425II, output power = 400 mW at $\lambda_0 = 532$ nm) as light source was used. The refractive index increment (dn/dC) was determined in the THF/H₂O (1:100) mixture at 25 °C by a differential refractometer.¹⁵ The details of LLS instrumentation and theory can be found elsewhere.^{16,17}

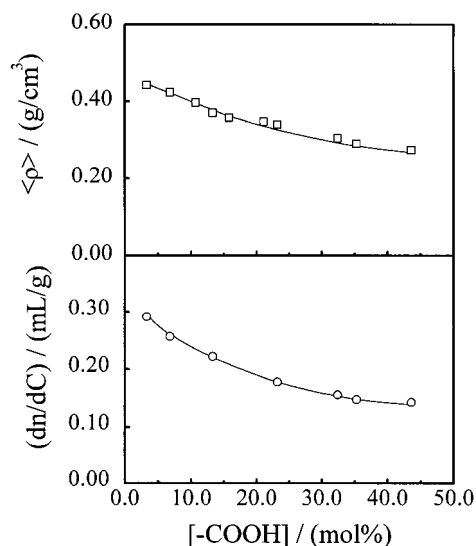


Figure 4. Carboxylation extent dependence of apparent chain density ($\langle \rho \rangle$) and specific refractive index increment (dn/dC) of CSEBS nanoparticles, where $dn/dC = \lim_{C \rightarrow 0} [(n_{\text{solution}} - n_{\text{solvent}})/C]$ and $\langle \rho \rangle = M_w/[^{4/3}N_A \langle R_h \rangle^3]$ with n , M_w , and $\langle R_h \rangle$ being refractive index, weight-average molar mass, and average hydrodynamic radius, respectively.

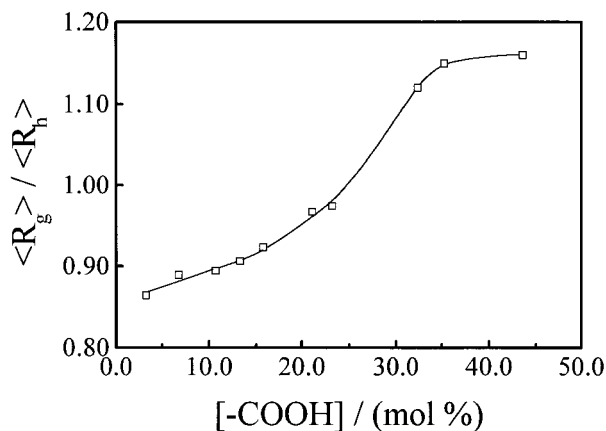


Figure 5. Carboxylation extent dependence of ratio of average radius of gyration to average hydrodynamic radius ($\langle R_g \rangle / \langle R_h \rangle$) of CSEBS nanoparticles, where $C = 1.0 \times 10^{-5}$ g/mL.

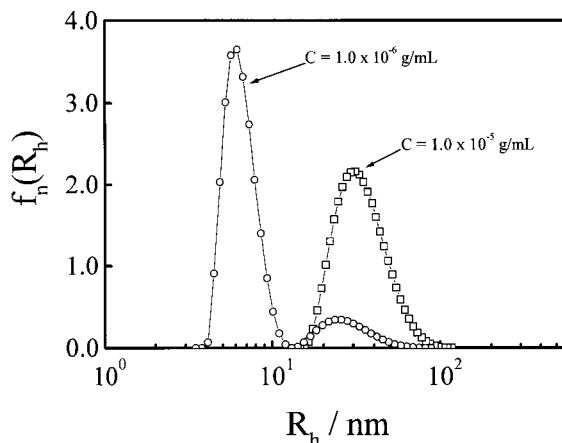


Figure 6. Effect of dilution on number distribution $f_n(R_h)$ of hydrodynamic radius of CSEBS nanoparticles, where $[-\text{COOH}] = 35.2$ mol %.

In static LLS, the angular dependence of the excess absolute time-averaged scattering light intensity, known as the excess Rayleigh ratio $R_{v,v}(q)$, of dilute polymer solutions with different concentrations (C) can lead to the weight-average molar mass

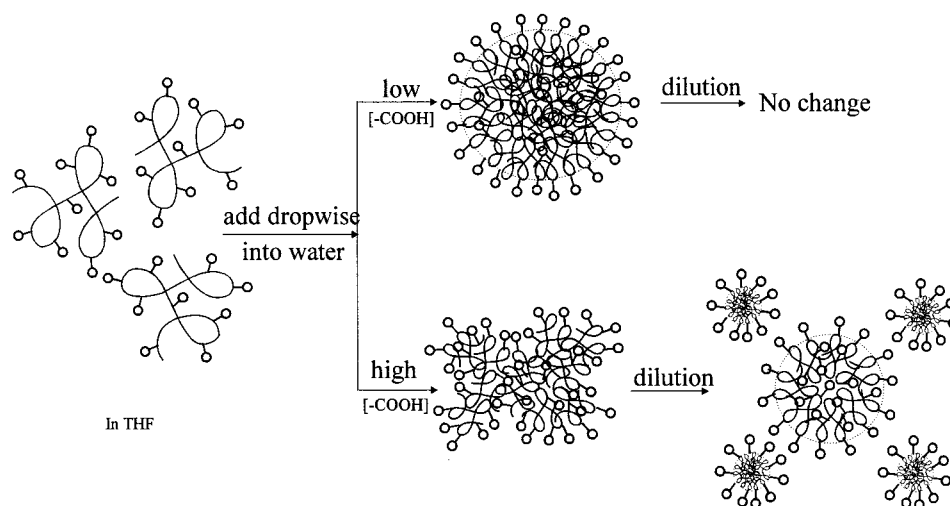


Figure 7. Schematic of CSEBS nanoparticle formation via a microphase inversion and effect of dilution on particle structure.

(M_w), the second virial coefficient (A_2), and the root-mean square z -average radius of gyration of the polymer chain in solution ($\langle R_g^2 \rangle^{1/2}$ or written as $\langle R_g \rangle$), where q is the scattering vector. In dynamic LLS, the Laplace inversion of a measured intensity–intensity time correlation function $G^{(2)}(q, t)$ in the self-beating mode is related to a line-width distribution $G(\Gamma)$.^{17,18} For a diffusive relaxation, $(\Gamma/q^2)_{C \rightarrow 0, q \rightarrow 0} \rightarrow D_0$. $G(\Gamma)$ can be converted into a transitional diffusion coefficient distribution $G(D_0)$ or a hydrodynamic radius distribution $f(R_h)$ via the Stokes–Einstein equation, $R_h = (k_B T / 6\pi\eta) D^{-1}$, where k_B , T , and η are the Boltzmann constant, the absolute temperature, and the solvent viscosity, respectively. All the LLS measurements were done at 25.0 ± 0.1 °C. The CSEBS dispersions were clarified using a $0.5 \mu\text{m}$ Millipore filter. Note that the concentration is so low that the extrapolation of $C \rightarrow 0$ is not necessary.

Results and Discussion

Figure 1 shows that the hydrophobic association of the CSEBS chains in water leads to surfactant-free polymeric nanoparticles. The relative distribution width is in the range 0.04–0.1. The narrow distribution with only one peak indicates that all CSEBS chains exist in aggregate form at the concentration ($C = 1.0 \times 10^{-5}$ g/mL). As expected, the particle size decreases as $[-\text{COOH}]$ increases because more carboxylic groups can stabilize more surface area, in that for a given mass of polymer smaller particles can provide more total surface area. Such formed CSEBS nanoparticles were very stable even after the dispersion was concentrated 100 times from 1.0×10^{-5} to 1.0×10^{-3} g/mL by solvent evaporation as shown in Figure 2. The driving force behind the stabilization of polymeric colloidal particles in water has long been debated. Langmuir¹⁹ suggested that the hydration or structural force of water molecules bounded on particle surfaces was responsible for the stabilization. Recently, Israelachvili and Wennerstrom²⁰ found that the hydration forces are not monotonically repulsive but attractive or oscillatory so that the stabilization of polymeric colloidal particles should be related to the entropic repulsion depending on the surface characteristics.

In the microphase inversion, the mixing of THF with water was nearly instant after each drop of the THF solution was added. The intrachain contraction and interchain association of the hydrophobic middle poly(ethylene-*co*-butylene) (EB) blocks lead to the particle formation, while the relatively more hydrophilic car-

boxylated polystyrene (CPS) blocks has a tendency to stay on the periphery. The number of carboxylic groups (n) on each nanoparticle surface increases as the association proceeds, and n is proportional to the average number of the polymer chains inside each nanoparticle (N_{chain}). On the other hand, the average particle volume (V) is also proportional to N_{chain} if the particle density is assumed to be a constant, so that $n \propto V \propto R^3$, where R is the particle size. Note that the particle surface area (S) is only proportional to R^2 . Therefore, $S/n \sim R^{-1}$; namely, the surface area stabilized per carboxylic group decreases as R increases until S/n reaches a minimum at which the interchain association stops. Further fusion of two such formed particles would be difficult, if not impossible, because the polymer chains are practically “frozen” inside due to strong hydrophobic interaction. The time required for an interparticle diffusion of the polymer chains is much longer than the collision time of two particles under Brownian motion in the dispersion. This is why the metastable nanoparticles are very stable in water.

Figure 3 shows that in the range 3.3–23.2 mol % both the particle size and the average number of polymer chains inside each nanoparticle (N_{chain}) decrease as $[-\text{COOH}]$ increases because the copolymer chains become more hydrophilic. Polymeric nanoparticles made of carboxylated and sulfonated polystyrene ionomers,¹⁰ poly(*N*-isopropylacrylamide) grafted with poly(ethylene oxide)²³ and poly(*N*-isopropylacrylamide-*co*-acrylic acid),²⁴ exhibit a similar tendency. Note that a small amount of $-\text{COOH}$ groups exist as $-\text{COO}^-$ and H^+ . The dissociation makes the chains more hydrophilic. As expected, less chains with a higher $[-\text{COOH}]$ can offer an equivalent number of stabilizing groups as more chains with a lower $[-\text{COOH}]$. The particle size is determined by a delicate balance between the hydrophobic attraction and hydrophilic stabilization (including electrostatic repulsion). Further increase of $[-\text{COOH}]$ in the range 23.2–43.6 mol % leads to a slight increase of $\langle R_h \rangle$ from 22 to 28 nm, but N_{chain} remains to be almost a constant, indicating the swelling of the particles.

Figure 4 shows that the average density (ρ) of the CSEBS particles decreases as $[-\text{COOH}]$ increases. Note that some of the carboxylic groups were inevitably trapped inside.²¹ A recent study of the aggregation of poly(ethylene-*co*-methacrylic acid) in water suggested

that each aggregate consisted of a hydrophobic core, an intermediate layer made of the ionomer chains and counterions, and a hydrophilic periphery where most of the ionic groups were located.²² The decrease of $\langle\rho\rangle$ as $[-\text{COOH}]$ increases can be attributed to the hydrophilic and electrostatic repulsion between the carboxylic groups inside. The decrease of dn/dC as $[-\text{COOH}]$ increases shown in Figure 4 reflects the association of more water molecules (a lower refractive index) with the CSEBS chains inside particles. The structure change of the nanoparticles can be better viewed in terms of the ratio of the average radius of gyration to the average hydrodynamic radius $\langle R_g \rangle / \langle R_h \rangle$.^{25,26}

Figure 5 shows that $\langle R_g \rangle / \langle R_h \rangle$ increases from ~ 0.86 to 1.16 as $[-\text{COOH}]$ increases from 3.3 to 43.6 mol % because $\langle R_h \rangle$ decreases fast than $\langle R_g \rangle$. It is known that for a uniform nondraining sphere, a hyperbranched cluster, and a random coil the ratios of $\langle R_g \rangle / \langle R_h \rangle$ are 0.774, ~ 1.0 – 1.3 , and ~ 1.5 – 1.8 , respectively.^{25–28} The fact that $\langle R_g \rangle / \langle R_h \rangle \sim 0.86$ at $[-\text{COOH}] \sim 3.3\%$ indicates that particles are practically draining and sphere-like. The increase of $\langle R_g \rangle / \langle R_h \rangle$ reveals that the nanoparticle structure gradually changes from sphere-like to cluster-like. The change in the particle structure was also evidenced by the effect of diluting the dispersion on $f(R_h)$. When $[-\text{COOH}] < 23.2$ mol %, the dilution had no influence on $f(R_h)$ because a relatively strong hydrophobic attraction holds the polymer chains together. However, when $[-\text{COOH}]$ is higher and the polymer chains are more hydrophilic, the dilution from 1.0×10^{-5} to 1.0×10^{-6} g/mL can split a narrowly distributed $f(R_h)$ into a bimodal distribution as shown in Figure 6. The peak related to the aggregates shifts to the left. Note that the x -axis is actually $\log(R_h)$ so that the small shift reflects a large decrease in size. The peak located at ~ 6 nm can be attributed to individual collapsed CSEBS chains since individual SEBS chains in THF (a good solvent) have a value of $\langle R_h \rangle \sim 13$ nm.²⁹ Therefore, in a very dilute dispersion, the interchain association is greatly suppressed so that individual collapsed chains are in equilibrium with large interchain aggregates, as schematically shown in Figure 7.

In conclusion, the self-assembly of carboxylated poly(styrene-*b*-ethylene-*co*-butylene-*b*-styrene) chains in water via the microphase inversion is governed by a delicate balance between intrachain contraction and interchain association. The hydrophobic attraction leads to, on one hand, the formation of polymeric particles, but on the other hand, the prevention of interparticle fusion. The hydrophilic repulsion results in, on one hand, the stabilization of the particles but, on the other hand, the swelling of the particles from sphere-like to hyperbranch-like. A right balance of the two different interactions enables us to prepare small surfactant-free polymeric nanoparticles stable in water.

Acknowledgment. The financial support of the National Basic Research Project—"Macromolecular Condensed State Program", the National Natural Science Foundation of China (NNSFC No. 29992590), the National Distinguished Young Investigator Grant (1996, 29625410), and the Research Grants Council of Hong Kong Government Earmarked Grant 1998/1999 (CUHK4123/98p, 2160111) is gratefully acknowledged. The Open Laboratory of Bond-Selective Chemistry in USTC provided a laser light scattering facility.

References and Notes

- Ben-Naim, A. *Hydrophobic Interactions*; Plenum Press: New York, 1980.
- Tanford, C. *The Hydrophobic Effect: Formation of Micelle and Biological Membrane*; Wiley-Interscience: New York, 1973.
- Kauzmann, W. *Adv. Protein Chem.* **1959**, *14*, 1.
- Jiang, X. K. *Acc. Chem. Res.* **1988**, *21*, 362.
- Ringsdorf, H.; Venzmer, J.; Winnik, F. *Macromolecules* **1991**, *24*, 1678.
- Zhang, Y. X.; Da, A. H.; Butler, G. B.; Hogen-Esch, T. E. *J. Polym. Sci., Polym. Chem. Ed.* **1992**, *30*, 1383.
- Zhang, L.; Eisenberg, A. *Science* **1995**, *268*, 1728.
- Eckert, A. R.; Webber, S. E. *Macromolecules* **1996**, *29*, 560.
- Gao, B.; Wesslen, B.; Wesslen, K. B. *J. Polym. Sci., Polym. Chem.* **1992**, *30*, 1799.
- Li, M.; Jiang, M.; Zhu, L.; Wu, C. *Macromolecules* **1997**, *30*, 220. Li, M.; Jiang, M.; Wu, C. *J. Polym. Sci., Polym. Phys.* **1997**, *35*, 1593. Li, M.; Zhang, Y.; Jiang, M.; Zhu, L.; Wu, C. *Macromolecules* **1998**, *31*, 6841.
- Olea, A. F.; Thomas, J. K. *Macromolecules* **1989**, *22*, 1165 and references therein.
- Marinsky, J. *J. Phys. Chem.* **1985**, *89*, 5294.
- Hird, B.; Eisenberg, A. *J. Polym. Sci., Polym. Chem.* **1993**, *31*, 1337.
- Liu, L.; Jiang, M. *Macromolecules* **1995**, *28*, 8702.
- Wu, C.; Xia, K. Q. *Rev. Sci. Instrum.* **1994**, *65*, 587.
- Zimm, B. H. *J. Chem. Phys.* **1948**, *16*, 1099.
- Berne, B. J.; Pecora, R. *Dynamic Light Scattering*; Plenum Press: New York, 1976.
- Chu, B. *Laser Light Scattering*, 2nd ed.; Academic Press: New York, 1991.
- Langmuir, I. *J. Chem. Phys.* **1938**, *6*, 873.
- Israelachvili, J.; Wennerstrom, H. *Nature* **1996**, *379*, 219.
- Ceska, G. W. *J. Appl. Polym. Sci.* **1974**, *18*, 427.
- Szajdzinska-Peitek, E.; Wolszczak, M.; Plonka, A.; Schlick, S. *J. Am. Chem. Soc.* **1998**, *120*, 4215.
- Qiu, X.; Kwan, C. M. S.; Wu, C. *Macromolecules* **1997**, *30*, 6090.
- Qiu, X.; Wu, C. *Macromolecules* **1997**, *30*, 7921.
- Buchard, W. In *Light Scattering Principles and Development*; Brown, W., Ed.; Clarendon Press: Oxford, 1996; p 439.
- Burchard, W.; Schmidt, M.; Stockmayer, W. H. *Macromolecules* **1980**, *13*, 1265.
- Douglas, J. P.; Roovers, J.; Freed, K. F. *Macromolecules* **1990**, *23*, 4168.
- Vagberg, L. J. M.; Cogan, K. A.; Gast, A. P. *Macromolecules* **1991**, *24*, 1670.
- Wu, C.; Woo, K.; Jiang, M. *Macromolecules* **1996**, *29*, 5361.

MA000530F